

Durham Research Online

Deposited in DRO:

27 January 2017

Version of attached file:

Accepted Version

Peer-review status of attached file:

Peer-reviewed

Citation for published item:

Pope, E. L. and Talling, P. J. and Carter, L. and Clare, M. A. and Hunt, J. E. (2017) 'Damaging sediment density flows triggered by tropical cyclones.', *Earth and planetary science letters*, 458 . pp. 161-169.

Further information on publisher's website:

<https://doi.org/10.1016/j.epsl.2016.10.046>

Publisher's copyright statement:

© 2016. This manuscript version is made available under the CC-BY-NC-ND 4.0 license
<http://creativecommons.org/licenses/by-nc-nd/4.0/>

Additional information:

Use policy

The full-text may be used and/or reproduced, and given to third parties in any format or medium, without prior permission or charge, for personal research or study, educational, or not-for-profit purposes provided that:

- a full bibliographic reference is made to the original source
- a [link](#) is made to the metadata record in DRO
- the full-text is not changed in any way

The full-text must not be sold in any format or medium without the formal permission of the copyright holders.

Please consult the [full DRO policy](#) for further details.

Damaging sediment density flows triggered by tropical cyclones

Ed L. Pope^{1,2*}, Peter J. Talling^{1,3}, Lionel Carter⁴, Michael A. Clare¹, James E. Hunt¹

¹*National Oceanography Centre, University of Southampton Waterfront Campus, European Way, Southampton, SO14 3ZH, UK.*

²*Department of Geography, Durham University, Science Laboratories, South Road, Durham, DH1 3LE, UK.*

³*Departments of Earth Science and Geography, Durham University, Science Laboratories, South Road, Durham, DH1 3LE, UK.*

⁴*Antarctic Research Centre, Victoria University of Wellington, Wellington, New Zealand.*

Abstract

The global network of subsea fibre-optic cables plays a critical role in the world economy and is considered as strategic infrastructure for many nations. Sediment density flows have caused significant disruption to this network in the recent past. These cable breaks represent the only means to actively monitor such flows over large oceanic regions. Here, we use a global cable break database to analyse tropical cyclone triggering of sediment density flows worldwide over 25 years. Cable breaking sediment density flows are triggered in nearly all areas exposed to tropical cyclones but most occur in the NW Pacific. They are triggered by one of three sets of mechanisms. Tropical cyclones directly trigger flows, synchronous to their passage, as a consequence of storm waves, currents and surges. Cyclones also trigger flows indirectly, with near-synchronous timing to their passage, as a consequence peak flood discharges. Last, cyclones trigger flows after a delay of days as a consequence of the failure of large volumes of rapidly deposited sediment. No clear relationship emerges between tropical cyclone activity (i.e. track, frequency and intensity) and the number of sediment density flows triggered. This is a consequence of the short period of observation. However,

expansion of the cable network and predicted changes to cyclone activity in specific regions increases the likelihood of increasing numbers of damaging flows.

Keywords

Sediment density flows; cable breaks; tropical cyclones; climate change; hazards

*Corresponding Author – Ed.Pope@noc.soton.ac.uk

1. Introduction

Tropical cyclones are common in many regions of the world and affect nearly all tropical areas (Emanuel, 2005). Associated with these meteorological phenomena are extreme winds, torrential rains and subsequent river floods, increased surface run-off and/or landslides, large waves and damaging storm surges leading to coastal flooding (Peduzzi et al., 2012). An often unrecognised hazard is that posed to subsea infrastructure by cyclone-triggered sediment density flows.

Sediment density flows (a generic term used here to encompass turbidity currents, debris flows, hyperpycnal plumes and submarine landslides, etc.) can travel at speeds of up to 19 ms^{-1} and runout for several hundreds of kilometres. These flows can damage critical seafloor infrastructure, such as that associated with the offshore hydrocarbon industry or subsea telecommunication cable networks (Carter et al., 2009; Pope et al., 2016). The seafloor telecommunication network currently carries >95% of global data and internet traffic making it integral to the global economy and strategic infrastructure for many countries (Carter et al., 2009; Burnett et al., 2013). Determining the timing and triggering of these flows is important for submarine geohazard assessment, especially whether their frequency may change as the oceans warm due to predicted climate change (Stocker, 2014).

Multiple triggering mechanisms have been identified for sediment density flows. These include earthquakes, tsunamis and storm wave loading, rapid sediment deposition and oversteepening,

direct plunging of dense river water (hyperpycnal flows) and volcanic activity (Piper and Normark, 2009). However, we have limited understanding of the frequency of flows worldwide or how often they are triggered by specific mechanisms because their exact timing and character are often problematic to measure. In most cases where a specific triggering mechanism has been identified, it has been based on cable breaks or damage to other seafloor infrastructure (e.g. Hsu et al., 2008; Cattaneo et al., 2012; see Talling et al., 2013 for more detail). This is particularly true of triggering of sediment density flows by tropical cyclones (Bea et al., 1983; Dengler et al., 1984; Alvarado, 2006; Carter et al., 2012; Gavey et al., 2016).

Using a global database of cable breaks, here we specifically focus on the role tropical cyclones play in triggering damaging sediment density flows. Furthering previous spatially and temporally restricted studies; the use of a global compilation of cable breaks allows the identification of areas where damaging sediment density flows, triggered by cyclones occur and how frequent these events have been globally over a 25 year time period.

1.2. Aims

Three main questions are addressed. First, how important are tropical cyclones for causing cable breaks on a global basis, and in which settings (submarine canyons, etc.) and water depths do cyclone induced breaks occur? Second, can the mechanisms by which cyclones trigger sediment density flows be identified from cable breaks? For example, are flows triggered by storm waves and currents during the tropical cyclone and/or are flows typically delayed and triggered a few days after the passing of the tropical cyclone (Carter et al., 2012)? Third, is the frequency of cyclone-triggered sediment density flows and cable breaks likely to change due to projected climate change?

2. Data and methods

2.1. Cable break database

This study is based on non-public, aggregated data supplied by Global Marine Systems Limited (UK) on a non-disclosure basis. The database contains information on the location of each subsea cable when it was laid (Fig. 1). It includes other installation information such as seabed type and duration the cable has been in service. Cable breaks within the database are identified and generally related to likely causes, i.e. seismic, trawling, anchor, etc. Each ‘break’ refers to a break or failure along a section of a specific cable. A ‘break’ can range from internal damage of the power conductor or optical fibres to the complete physical separation of the entire cable assembly. Each recorded ‘break’ may therefore also represent multiple breaks along a single section of cable. The timing of a break in the database is recorded to the nearest day.

2.2. Tropical cyclone data

2.2.1. Tropical cyclone track data

Historical tropical cyclone track data were obtained from the National Hurricane Center (NHC) Hurdad-2 “best track” dataset (Landsea et al., 2013). This dataset is an archive compiled every 6 hours (at 0000, 0600, 1200, 1800 UTC) and includes reports of storm position and maximum wind speeds.

2.2.2. Tropical cyclone characterisation: ECMWF ERA-interim reanalysis data

The global coverage of ocean buoys recording variables such as surface pressure and wave height is spatially variable, and such data are not always freely available. The same is true of terrestrial weather stations. Thus to analyse specific tropical cyclone characteristics we used global model data in order to homogenise data quality. Records of tropical cyclone characteristics came from ERA-Interim global atmospheric reanalysis produced by the European Centre for Medium-Range Weather Forecasts (Dee et al., 2011). ERA-Interim covers the period from 1 January 1979 onwards, and continues to be extended forward in near-real time. 3-hourly estimates of surface pressure (Pa),

significant wave height (m), total precipitation (m) and surface runoff (m) data were obtained from the ERA-interim model. These data were gridded at a spatial resolution of $0.125^{\circ} \times 0.125^{\circ}$.

2.3. Comparison of cable break and tropical cyclone databases

All cable breaks within the database attributed to the following causes were included in our analysis: earthquakes, landslides, chafe under current action, other natural causes, and unknown causes. Among these categories, cable breaks with a known cause unrelated to tropical cyclones were removed, such as those due to earthquakes (Pope et al., 2016). A tropical cyclone was attributed to be the cause of a sediment density flow if the cable break coincided with the passing of a tropical cyclone according to the best-track data and the ERA-interim data, or occurred within 14 days of the end of a related river discharge peak if no other apparent triggers could be found.

Where a tropical cyclone appears to have triggered a sediment density flow, local environmental variables were extracted from the ERA-Interim data. Where a cable break occurred beyond the continental shelf edge, surface pressure and significant wave height measurements were measured at the nearest point on the shelf edge. Where a cable break occurred on the shelf itself, surface pressure and significant wave height were measured at the location of the cable break. Total precipitation was measured at the nearest terrestrial location to each cable break; the maximum distance was 260 km on the Mississippi Fan (mean distance of all the breaks; 95 km).

Breaks were attributed to by specific triggers depending on the timing of the break itself. A cable break was specified as Type 1 if it occurred during the initial passing of the tropical cyclone and coincided with rising or peaking significant wave heights, or a drop in surface pressure (Fig. 2). A Type 2 cable break occurred after the peak in significant wave height, but coincident with the peak in river flood discharges (Fig. 2). A Type 3 cable break followed the peak in cyclone-related river flood discharge (Fig. 2). The time limit set for this was 14 days as a consequence of the variable flood hydrographs, which can occur (Williams, 1969). Flood hydrographs can vary between different

basins as a consequence of the different shape and size of individual basins but also as a consequence of differing relief and land-use patterns (Woods and Sivapalan, 1999). They can also vary in shape in the same basin at different times according to different antecedent conditions. It must also be acknowledged that as time between the hydrograph peak and the cable break occurring increases, it become increasingly difficult to directly link the occurrence of a cable break to the passage of the tropical cyclone rather than a separate mechanism. However, no obvious trigger, such as an earthquake was observed in these cases.

3. Results

Globally, between January 1989 and January 2015, there were 35 cable breaks that could potentially be attributed to tropical cyclone activity (Table 1). Cables broke in water depths of between 20 m and 6120 m, of which 19 cables broke at water depths >2000 m. The largest number of breaks was found offshore Taiwan; here 20 cable breaks were associated with tropical cyclones (Fig. 3a). There were also 3 cable breaks off Japan and 1 off the Philippines (Fig. 3a). In the Indian Ocean, tropical cyclone-related breaks were found offshore Madagascar (1 break) and La Reunion (6 breaks; Fig. 3b). Elsewhere 3 breaks were found to have occurred in the Caribbean Sea and 1 break in the Eastern Pacific (Fig. 3c).

The 35 cable breaks in the dataset were caused by 22 separate tropical cyclones. Multiple breaks were caused by three tropical cyclones. Typhoon Sinlaku was the potential cause of 2 cable breaks off East Taiwan in 2002. Cyclone Gamede was associated with 2 cable breaks offshore La Reunion in 2007. Typhoon Morakot resulted in 10 cable breaks. This number differs from previous studies of Typhoon Morakot, which recorded “at least nine” cable breaks (Carter et al., 2012; Gavey et al., 2016) as a consequence of additional data.

The 35 cable breaks potentially associated with tropical cyclones are found in several distinct environmental settings (Table 1). The largest number of cable breaks (22) are found in or closely

associated with submarine canyons. Most of these are offshore Taiwan (19); others occurred offshore the Philippines and Madagascar. The second most common location (9) for cable breaks is close to river mouths or on associated deep-sea fans where turbidity currents are known to occur (i.e. the Mississippi Fan, the Yellahs Fan). Of these, 6 are located within the sediment wave fields of the Mafate and Saint-Denis Fans offshore La Reunion. The remainder of cable breaks (4) occurred on open continental shelves and deep sea fans.

Assuming that each cable-breaking flow originated at the head of their associated submarine canyon or at the mouth of close-by rivers, cables were broken at distances of between 1 and 384 km from their source. The environmental settings of the cable breaks suggests that the majority of cable-breaking sediment flows triggered by tropical cyclones began in areas where large volumes of sediment had previously accumulated, such as in the heads of submarine canyons. They also suggest that most damaging flows were channelized. Channelization likely increased the probability that the flow would have sufficient power to break a cable, thus increasing the likelihood of detection in the cable break database.

The timing of the 35 cable breaks relative to the passing of a tropical cyclone is highly variable (Table 1). Peaks in significant wave height and drops in surface pressure as the tropical cyclone passed correspond to 4 cable breaks; each break was associated with an individual storm. Fig. 4 shows the timing of a cable break coincident with the initial passing of Severe Tropical Storm Utor offshore Taiwan in 2001. Tropical cyclone precipitation-related peaks in river discharge were associated with 13 cable breaks (Fig. 5). Both breaks associated with Cyclone Gamede were related to river discharge. Most cable breaks (18) occurred following a delay from peak flood discharge of at least 2 days (Figs. 6 and 7). The longest delay was 12 days after river discharge had returned to pre-cyclone levels (20 days after the peak discharge). Cable breaks associated with delays were associated with 9 tropical cyclones.

4. Discussion

4.1. Tropical cyclone triggering of sediment density flows

4.1.1. Type 1 breaks: Direct and synchronous triggering of sediment density flows

The cable break database shows that sediment density flows can be triggered (Type 1) during the initial passing of a tropical cyclone (Figs. 4 and 7b). We attribute a Type 1 break to slope failure and run-out triggered most likely by dynamic loading of the seafloor. Dynamic loading is the result of storm waves, storm surges or internal waves occurring during a tropical cyclone (Prior et al., 1989; Wright and Rathje, 2003). These breaks are attributed to dynamic loading-triggered sediment density flows and not wave action alone because the breaks occur well below the wave base; at depths greater than 1200 m (see Table 1). However, the lack of sequential breaks as seen in other studies (Carter et al., 2012; Cattaneo et al., 2012; Gavey et al., 2016) means we cannot rule out other causes.

Storm surges are generated by a combination of wind stresses and reduced atmospheric pressure (Karim and Mimura, 2008). At the continental shelf edge, the advance of a storm surge can exert large hydrodynamic pressures on the seafloor and elevate subsurface pore pressures (Zhang et al., 2015). Such transient changes can promote slope instability and its run-out (Bea et al., 1983; Wright and Rathje, 2003).

Storm waves can trigger sediment density flows through two processes. First, they can alter pore pressures through dynamic loading. Passing wave crests increase pore pressures, while wave troughs generate seepage pressures (Seed and Rahman, 1978). Where sediment lacks rigidity or has low permeability, pore water pressures are able to progressively build or migrate laterally through the sediment. Over time this can cause liquefaction or the rupture of inter-particle cohesive bonds (Puig et al., 2008) leading to sediment failure (Lamb and Parsons, 2005). Second, the orbital motion of the water particles can impart horizontal shear on the seabed (Jeng and Seymour, 2007). Where the sediment shear strength is insufficient to resist the shear stress, failure and sediment transport can

occur in the form of plane shear, liquefied flow sliding or slope failure (Lambrechts et al., 2010). Horizontal shear stresses induced by cyclone-forced currents can induce failure of weak sediments in the same way (Alford, 2003).

The limited number (4 breaks) of Type 1 events compared to other break types suggests that dynamic loading itself does not trigger large numbers of long run-out and damaging sediment density flows. These processes are therefore likely to be more important for the entrainment and deposition of shelf sediments (Sullivan et al., 2003). Failures of the deposited sediment may then result from other triggers.

4.1.2. Type 2 breaks: Indirect and near-synchronous triggering

Type 2 cable breaks were three times more common (13 breaks) during the passage, or after the peak of, a tropical cyclone, but after coincident peaks in wave height, surface pressure and rainfall (Fig. 7c). Type 2 breaks are related to sediment density flows triggered by either cumulative effects (rather than the peak event as in Type 1) of storm wave/current activity, or indirectly as a consequence of peak river flood discharges resulting from tropical cyclone precipitation. Peak flood discharges often coincide with continued storm wave activity; hence isolation of a specific mechanism for Type 2 breaks is difficult from the cable break database alone. Typhoon Morakot (Fig. 5; Carter et al., 2012) is the best known example of a peak flood discharge trigger for a sediment density flow that lagged behind the peak intensity of the cyclone itself. Sufficiently large flood discharges can trigger sediment density flows either through the generation of hyperpycnal plumes (Parsons et al., 2001; Mulder et al., 2003; Piper and Normark, 2009) or through rapid deposition and subsequent remobilisation of river plume sediments (Parsons et al., 2001; Clare et al., 2016; Gavey et al., 2016). In both cases the initial flow entrains water and sediment; thus giving the flow sufficient energy to break a subsea cable (Fig. 7c).

4.1.3. Type 3 breaks: Indirect and delayed triggering

The largest number of cable breaks (18), occurred shortly after the passage of a tropical cyclone. Here, we suggest that these Type 3 breaks relate to processes that lag behind the passage of a tropical cyclone, but are still related to its residual effects (Figs 6 and 7d). Such lagged-triggering may be related to the deposition of large volumes of sediment during and immediately after a storm. Alternatively sediment at the shelf break or in canyon heads may have been destabilised by the cumulative effects of surface gravity waves and internal tide/wave effects (Lee et al., 2009).

Storm wave/current action and flood discharges can transport and deposit large volumes of sediment at the shelf edge or in canyon heads (Puig et al., 2004; Liu et al., 2009). The rate of deposition may depend on; (1) the extent to which the water column on the continental shelf has been stirred up by the passage of the cyclone (Sullivan et al., 2003) and; (2) the response and size of the nearby river basin (Chen et al., 2012). These aspects can lead to delayed failures due to oversteepening and loading by rapidly deposited sediment, and inhibited dissipation of excess pore pressures (Clare et al., 2016; Figs 6 and 7d).

Liquefaction related to storm waves may also cause delayed failures. Laboratory and field tests focussing on earthquake shaking have shown that soil liquefaction beneath silt laminae, beds or lenses present in sand layers can lead to the generation of water film layers (Scott and Zuckerman, 1972; Kokusho and Kojima, 2002). These water films can persist for several days after an earthquake, acting as sliding surfaces for delayed sediment failures (Özener et al., 2009). If storm waves cause liquefaction of seafloor sediments by the processes outlined in Section 4.1.1, then it is possible for water film layers to be generated. Delayed failures can subsequently occur following these water film layers.

4.1.4. Do delayed cable breaks result from other factors?

We now consider whether delayed cable breaks result from either the time taken for a sediment density flow to reach a cable or whether the flow is in fact triggered by a process unrelated to the tropical cyclone.

The time taken for a flow to reach a cable and be recorded as a cable break has inflated the delay times given. A significant number of cable breaks (12) were located more than 100 km from the likely initiation point for sediment density flows. Given reasonable flow speeds (Carter et al., 2012; Cattaneo et al., 2012; Gavey et al., 2016) and the distances between the likely point of initiation and the cable break, a delay of up to 2 days (48 hours) is likely. The format of the cable break database may contribute to this delay, as it only records the timing of each break to the nearest day.

Quantifying whether a cyclone triggered a sediment density flow following a long delay, i.e. more than 7 days, is more difficult. Prior to this study, delayed triggering of sediment density flows was observed in several locations (Hsu et al., 2008; Carter et al., 2012; Clare et al., 2016). These studies identified delays between peak discharge and the occurrence of a flow of between a few hours to a week. There are, however, no measurements of changing subsurface properties up until eventual failure in these previous studies or in this study. It is therefore difficult to precisely define the point at which deposited sediment will no longer fail as a consequence of cyclone forcing, and thus require an additional trigger. This should be the subject of future studies.

4.2. Will climate change make tropical cyclone triggered sediment density flows more likely?

Understanding whether the frequency of cyclone-triggered sediment density flows will increase as a consequence of climate change faces a number of challenges. First, possible trends in tropical cyclone activity remain uncertain as a consequence of the short period of accurate observation and the large amount of natural inter-annual variability (Knutson et al., 2010). This variability contributes to uncertainty in predictive modelling of different warming scenarios (Sugi et al., 2009; Knutson et al., 2010). Second, the number of fibre-optic cables and the diversity of cable locations have

increased due to growing reliance on this communications network (Carter et al., 2014; Pope et al., 2016). These factors complicate the interpretation of whether changes to the number of observed tropical cyclone triggered flows are a consequence of changes to tropical cyclone activity or to hazard exposure of the cable network. It is therefore difficult to make projections of trends in the number of cable breaks. One exception is the northwestern Pacific (Mei and Xie, 2016). Here, increasing cyclone intensity (Emanuel, 2005), poleward migration of storm tracks (Kossin et al., 2014) and slower tropical cyclone passage (Lee et al., 2015) have been linked to increased sediment discharge to the continental shelf (Lee et al., 2015; Mei and Xie, 2016). The likelihood that cyclones will trigger sediment density flows or at least precondition slopes to fail, triggered by other processes (e.g. earthquakes; Gavey et al., 2016; Pope et al., 2016) is thereby enhanced. Increased tropical cyclone activity does therefore appear to increase the likelihood of flow triggering.

5. Conclusions

Tropical cyclones trigger cable-breaking sediment density flows in almost all areas where cyclones occur globally. Cyclone-forced flows are particularly common around South East Asia, especially off Taiwan and the Philippines. Flows can be triggered by dynamic loading of the seabed through storm surge and storm-wave action, but are more commonly the result of fluvial flood discharge. Importantly, they are also triggered indirectly after a tropical cyclone has passed when large volumes of rapidly deposited fluvial and shelf sediment are prone to failure. Such deposits may be subject to delayed failure to form cable-damaging flows. It is unclear whether climate change will affect the global frequency of tropical cyclone triggered flows, but it is likely to increase the number of cable breaks in major cable corridors such as off Taiwan.

Acknowledgements

We are very grateful to Global Marine Systems Ltd. (GMSL) for access and permission to use its cable break database. In this regard, the assistance of Brian Perrat and Steve Holden of GMSL is

particularly appreciated. General information on subsea telecommunications cables was generously supplied by the International Cable Protection Committee and its members. We thank the British Atmospheric Data Centre and ECMWF for providing reanalysis data. This work was supported by two NERC Environmental Risks to Infrastructure Innovation Programme grants (NE/N012798/1 and NE/P009190/1). Talling was supported by a NERC Royal Society Industry Fellowship to understand submarine sediment flows and the risk they pose to global telecommunications. Clare was supported by a NERC Knowledge Exchange Fellowship to identify and fill the gaps in knowledge of environmental risks to infrastructure (NE/P005780/1). We would like to thank the editor Martin Frank, David Piper and an anonymous reviewer for their in depth reviews and comments which greatly improved this manuscript.

- Alford, M.H., 2003. Redistribution of energy available for ocean mixing by long-range propagation of internal waves. *Nature* 423, 159-162.
- Alvarado, A., 2006. Updates on MMS (Minerals Management Service) regulatory issues for offshore operators. Uniform Resource Locator (URL): <http://www.southerngas.org/EVENTS/documents/SGAOGO06Alvarado.pdf> (accessed 13 March, 2007).
- Bea, R.G., Wright, S.G., Sircar, P., Niedoroda, A.W., 1983. Wave-Induced Slides in South Pass Block 70, Mississippi Delta. *Journal of Geotechnical Engineering-Asce* 109, 619-644.
- Becker, J.J., Sandwell, D.T., Smith, W.H.F., Braud, J., Binder, B., Depner, J., Fabre, D., Factor, J., Ingalls, S., Kim, S.H., 2009. Global bathymetry and elevation data at 30 arc seconds resolution: SRTM30_PLUS. *Marine Geodesy* 32, 355-371.
- Burnett, D.R., Beckman, R., Davenport, T.M., 2013. *Submarine Cables: the handbook of Law and Policy*. Martinus Nijhoff Publishers.
- Carter, L., Burnett, D., Drew, S., Hagadorn, L., Marle, G., Bertlett-McNeil, D., Irvine, N., 2009. Submarine cables and the oceans- connecting the world: UNEP-WCMC Biodiversity Series 31. ICPC/UNEP/UNEP-WCMC. 64.
- Carter, L., Milliman, J.D., Talling, P.J., Gavey, R., Wynn, R.B., 2012. Near-synchronous and delayed initiation of long run-out submarine sediment flows from a record-breaking river flood, offshore Taiwan. *Geophysical Research Letters* 39.
- Carter, L., Gavey, R., Talling, P.J., Liu, J.T., 2014. Insights into submarine geohazards from breaks in subsea telecommunication cables. *Oceanography* 27, 58-67.
- Cattaneo, A., Babonneau, N., Ratzov, G., Dan-Unterseh, G., Yelles, K., Bracene, R., De Lepinay, B.M., Boudiaf, A., Déverchère, J., 2012. Searching for the seafloor signature of the 21 May 2003 Boumerdes earthquake offshore central Algeria. *Natural Hazards and Earth System Sciences* 12, 2159-2172.
- Chen, J.C., Huang, W.S., Jan, C.D., Yang, Y.H., 2012. Recent changes in the number of rainfall events related to debris-flow occurrence in the Chenyulan Stream Watershed, Taiwan. *Natural Hazards and Earth System Science* 12, 1539-1549.
- Clare, M.A., Hughes Clarke, J.E., Talling, P.J., Cartigny, M.J.B., Pratomo, D.G., 2016. Preconditioning and triggering of offshore slope failures and turbidity currents revealed by most detailed monitoring yet at a fjord-head delta. *Earth and Planetary Science Letters* 450, 208-220.
- Dee, D.P., Uppala, S.M., Simmons, A.J., Berrisford, P., Poli, P., Kobayashi, S., Andrae, U., Balmaseda, M.A., Balsamo, G., Bauer, P., Bechtold, P., Beljaars, A.C.M., van de Berg, L., Bidlot, J., Bormann, N., Delsol, C., Dragani, R., Fuentes, M., Geer, A.J., Haimberger, L., Healy, S.B., Hersbach, H., Hólm, E.V., Isaksen, I., Kållberg, P., Köhler, M., Matricardi, M., McNally, A.P., Monge-Sanz, B.M., Morcrette, J.J., Park, B.K., Peubey, C., de Rosnay, P., Tavolato, C., Thépaut, J.N., Vitart, F., 2011. The ERA-Interim reanalysis: configuration and performance of the data assimilation system. *Quarterly Journal of the Royal Meteorological Society* 137, 553-597.

Dengler, A.T., Wilde, P., Noda, E.K., Normark, W.R., 1984. Turbidity currents generated by Hurricane Iwa. *Geo-Marine Letters* 4, 5-11.

Emanuel, K., 2005. Increasing destructiveness of tropical cyclones over the past 30 years. *Nature* 436, 686-688.

Gavey, R., Carter, L., Liu, J.T., Talling, P.J., Hsu, R.T., Pope, E.L., Evans, G., 2016. Frequent sediment density flows formed by different triggering mechanisms: observations from subsea cable breaks in the Gaoping Canyon-Manila Trench, Taiwan. *Marine Geology*.

Hsu, S.K., Kuo, J., Lo, C.L., Tsai, C.H., Doo, W.B., Ku, C.Y., Sibuet, J.C., 2008. Turbidity Currents, Submarine Landslides and the 2006 Pingtung Earthquake off SW Taiwan. *Terrestrial Atmospheric and Oceanic Sciences* 19, 767-772.

Jeng, D.-S., Seymour, B.R., 2007. Simplified analytical approximation for pore-water pressure buildup in marine sediments. *Journal of Waterway Port Coastal and Ocean Engineering-Asce* 133, 309-312.

Karim, M.F., Mimura, N., 2008. Impacts of climate change and sea-level rise on cyclonic storm surge floods in Bangladesh. *Global Environmental Change* 18, 490-500.

Knutson, T.R., McBride, J.L., Chan, J., Emanuel, K., Holland, G., Landsea, C., Held, I., Kossin, J.P., Srivastava, A.K., Sugi, M., 2010. Tropical cyclones and climate change. *Nature Geoscience* 3, 157-163.

Kokusho, T., Kojima, T., 2002. Mechanism for postliquefaction water film generation in layered sand. *Journal of geotechnical and geoenvironmental engineering* 128, 129-137.

Kossin, J.P., Emanuel, K.A., Vecchi, G.A., 2014. The poleward migration of the location of tropical cyclone maximum intensity. *Nature* 509, 349-352.

Lamb, M.P., Parsons, J.D., 2005. High-density suspensions formed under waves. *Journal of Sedimentary Research* 75, 386-397.

Lambrechts, J., Humphrey, C., McKinna, L., Gource, O., Fabricius, K.E., Mehta, A.J., Lewis, S., Wolanski, E., 2010. Importance of wave-induced bed liquefaction in the fine sediment budget of Cleveland Bay, Great Barrier Reef. *Estuarine, Coastal and Shelf Science* 89, 154-162.

Landsea, C., Franklin, J., Beven, J., 2013. The revised Atlantic hurricane database (HURDAT2). United States National Oceanic and Atmospheric Administration's.

Lee, I.-H., Lien, R.-C., Liu, J.T., Chuang, W.S., 2009. Turbulent mixing and internal tides in Gaoping (Kaoping) submarine canyon, Taiwan. *Journal of Marine Systems* 76, 383-396.

Lee, T.-Y., Huang, J.-C., Lee, J.-Y., Jien, S.-H., Zehetner, F., Kao, S.-J., 2015. Magnified Sediment Export of Small Mountainous Rivers in Taiwan: Chain Reactions from Increased Rainfall Intensity under Global Warming. *PloS one* 10, e0138283.

Liu, J.T., Hung, J.J., Lin, H.L., Huh, C.A., Lee, C.L., Hsu, R.T., Huang, Y.W., Chu, J.C., 2009. From suspended particles to strata: The fate of terrestrial substances in the Gaoping (Kaoping) submarine canyon. *Journal of Marine Systems* 76, 417-432.

- Lu, J.Y., Hong, J.H., Su, C.C., Wang, C.Y., Lai, J.S., 2008. Field measurements and simulation of bridge scour depth variations during floods. *Journal of Hydraulic Engineering* 134, 810-821.
- Mei, W., Xie, S.P., 2016. Intensification of landfalling typhoons over the northwest Pacific since the late 1970s. *Nature Geoscience* 9, 753-757.
- Mulder, T., Syvitski, J.P.M., Migeon, S., Faugeres, J.-C., Savoye, B., 2003. Marine hyperpycnal flows: initiation, behavior and related deposits. A review. *Marine and Petroleum Geology* 20, 861-882.
- Özener, P.T., Özaydın, K., Berilgen, M.M., 2009. Investigation of liquefaction and pore water pressure development in layered sands. *Bulletin of Earthquake Engineering* 7, 199-219.
- Parsons, J.D., Bush, J.W.M., Syvitski, J.P.M., 2001. Hyperpycnal plume formation from riverine outflows with small sediment concentrations. *Sedimentology* 48, 465-478.
- Peduzzi, P., Chatenoux, B., Dao, H., De Bono, A., Herold, C., Kossin, J., Mouton, F., Nordbeck, O., 2012. Global trends in tropical cyclone risk. *Nature Clim. Change* 2, 289-294.
- Piper, D.J.W., Normark, W.R., 2009. Processes that initiate turbidity currents and their influence on turbidites: a marine geology perspective. *Journal of Sedimentary Research* 79, 347-362.
- Pope, E.L., Talling, P.J., Carter, L., 2016. Which earthquakes trigger damaging submarine mass movements: Insights from a global record of submarine cable breaks? *Marine Geology*.
- Prior, D.B., Suhayda, J.N., Lu, N.-Z., Bornhold, B.D., Keller, G.H., Wiseman, W.J., Wright, L.D., Yang, Z.-S., 1989. Storm wave reactivation of a submarine landslide. *Nature* 341, 47-50.
- Puig, P., Ogston, A.S., Mullenbach, B.L., Nitttrouer, C.A., Parsons, J.D., Sternberg, R.W., 2004. Storm-induced sediment gravity flows at the head of the Eel submarine canyon, northern California margin. *Journal of Geophysical Research: Oceans* 109.
- Puig, P., Palanques, A., Orange, D.L., Lastras, G., Canals, M., 2008. Dense shelf water cascades and sedimentary furrow formation in the Cap de Creus Canyon, northwestern Mediterranean Sea. *Continental Shelf Research* 28, 2017-2030.
- Scott, R.F., Zuckerman, K.A., 1972. Sandblows and liquefaction in the great Alaska earthquake of 1964. *Engineering Publication* 1606, 170-189.
- Seed, H.B., Rahman, M.S., 1978. Wave-induced pore pressure in relation to ocean floor stability of cohesionless soils. *Marine Georesources & Geotechnology* 3, 123-150.
- Stocker, T.F., 2014. *Climate change 2013: the physical science basis: Working Group I contribution to the Fifth assessment report of the Intergovernmental Panel on Climate Change*. Cambridge University Press.
- Sugi, M., Murakami, H., Yoshimura, J., 2009. A reduction in global tropical cyclone frequency due to global warming. *Sola* 5, 164-167.
- Sullivan, M.C., Cowen, R.K., Able, K.W., Fahay, M.P., 2003. Effects of anthropogenic and natural disturbance on a recently settled continental shelf flatfish. *Marine Ecology Progress Series* 260, 237-253.

450

451 Talling, P.J., Paull, C.K., Piper, D.J.W., 2013. How are subaqueous sediment density flows triggered,
452 what is their internal structure and how does it evolve? Direct observations from monitoring of
453 active flows. *Earth-Science Reviews* 125, 244-287.

454

455 Williams, J.R., 1969. Flood routing with variable travel time or variable storage coefficients.
456 *Transactions of the ASAE* 12, 100-0103.

457

458 Woods, R., Sivapalan, M., 1999. A synthesis of space-time variability in storm response: Rainfall,
459 runoff generation, and routing. *Water Resources Research* 35, 2469-2485.

460

461 Wright, S.G., Rathje, E.M., 2003. Triggering mechanisms of slope instability and their relationship to
462 earthquakes and tsunamis. *Pure and Applied Geophysics* 160, 1865-1877.

463

464 Zhang, M., Huang, Y., Bao, Y., 2015. The mechanism of shallow submarine landslides triggered by
465 storm surge. *Natural Hazards*, 1-11.

466

467

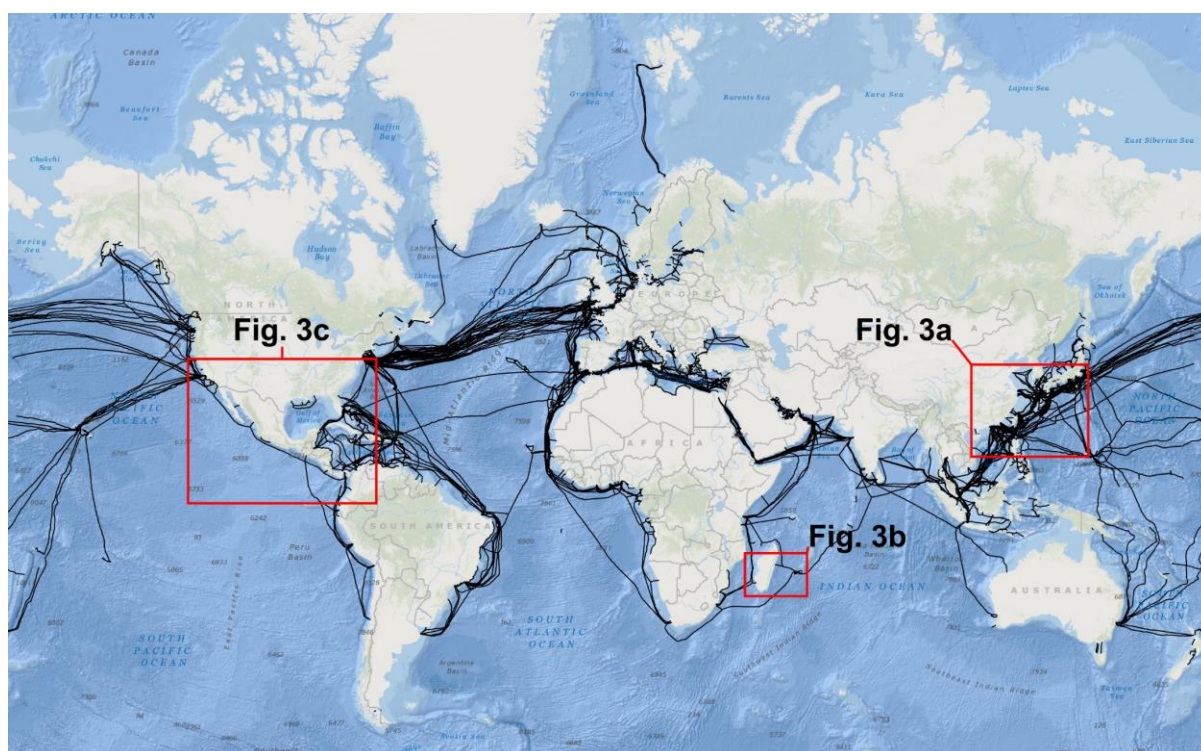
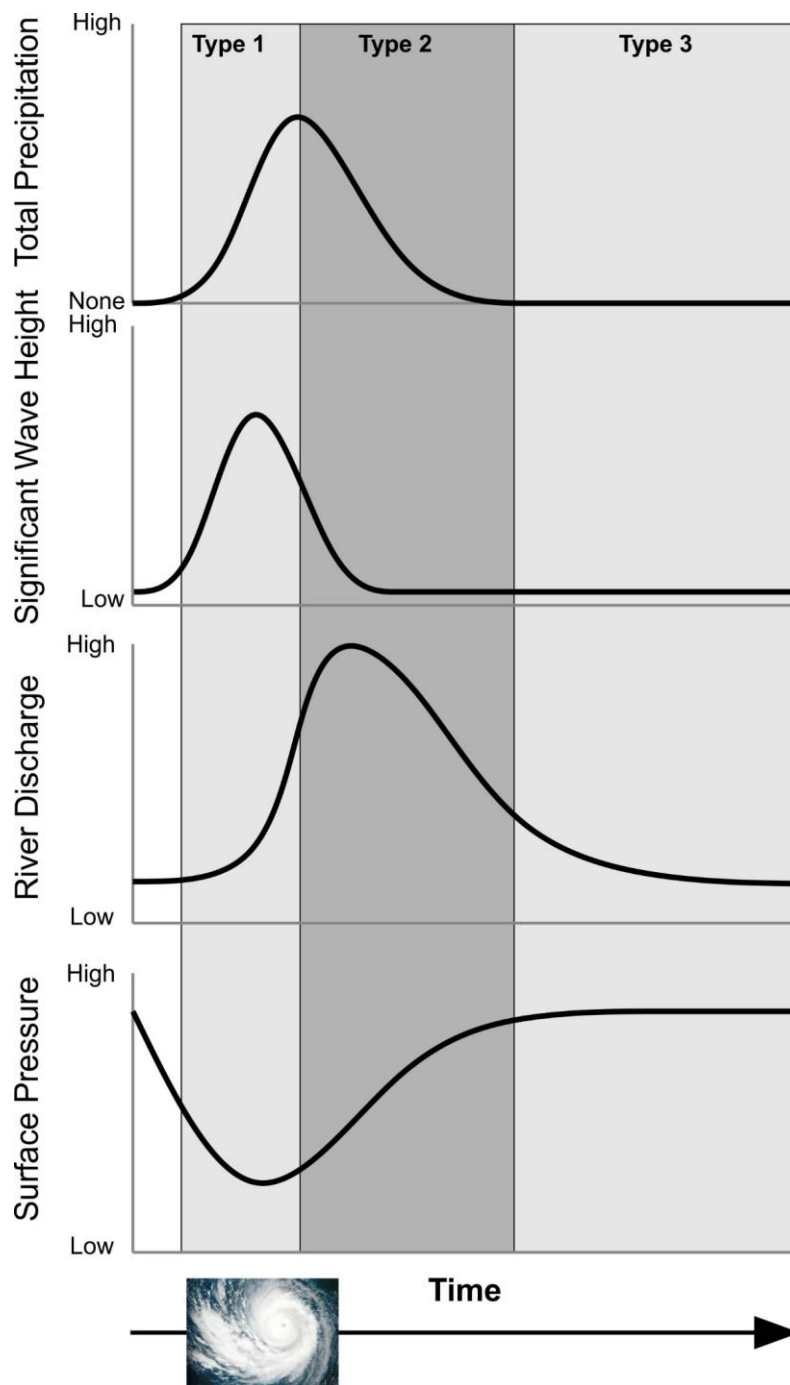
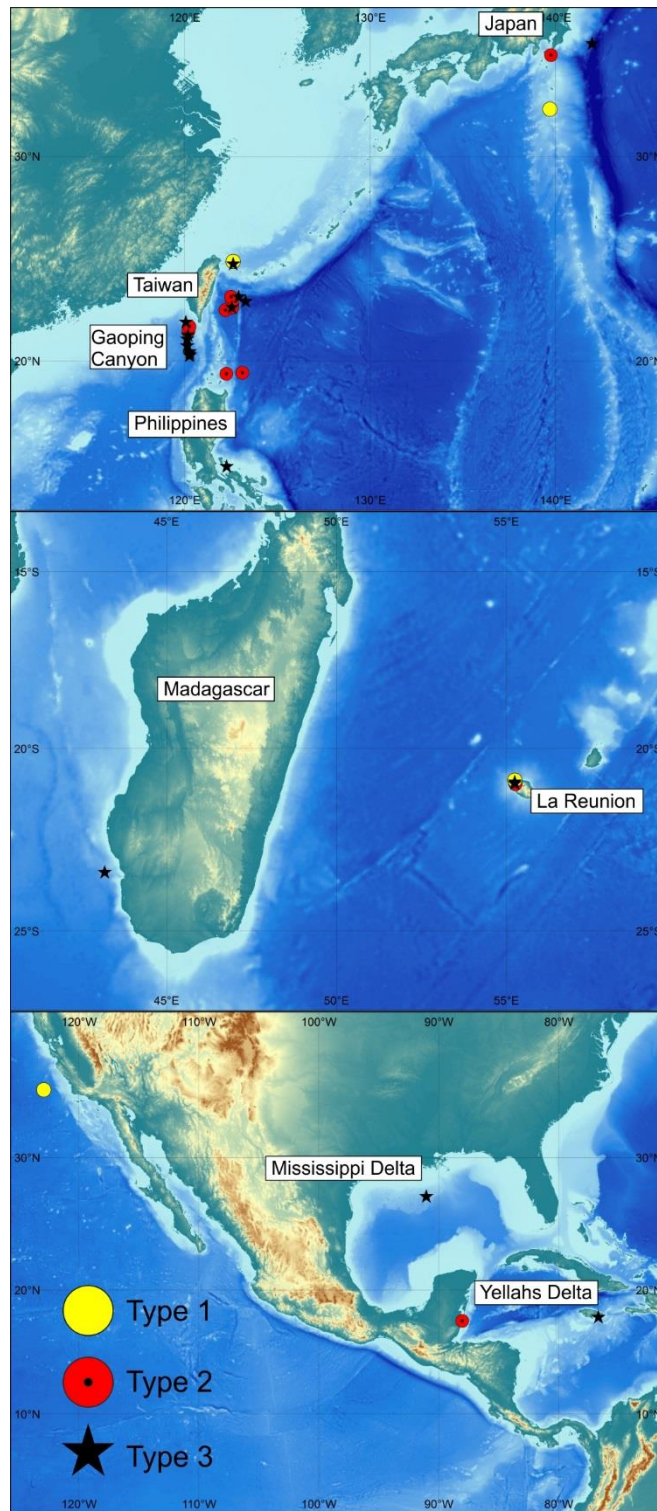


Fig. 1. Map of the submarine cable network used in this study.



472

473 Fig. 2. Idealised schematic of the relationship between environmental variables during the passage
 474 of a tropical cyclone and the timing of a cable break. Type 1 breaks are defined as occurring with
 475 rising and peaking significant wave heights and storm driven flows or the drop in surface pressure
 476 associated with the passage of a tropical cyclone. Type 2 occur after the peak in significant wave
 477 height but associated with the peak in river flood discharges. Type 3 occur if the break was within 14
 478 days of the peak in cyclone related river flood discharge.



479

480 Fig. 3. Locations of submarine cable breaks inferred to be associated with tropical cyclones. a) Cable
 481 breaks offshore Japan, Taiwan and the Philippines. b) Cable breaks offshore Madagascar and La
 482 Reunion. c) Cable breaks offshore the USA, Central America and the Caribbean Islands. Bathymetry
 483 and topographic data were obtained from the GEBCO database (Becker et al., 2009).

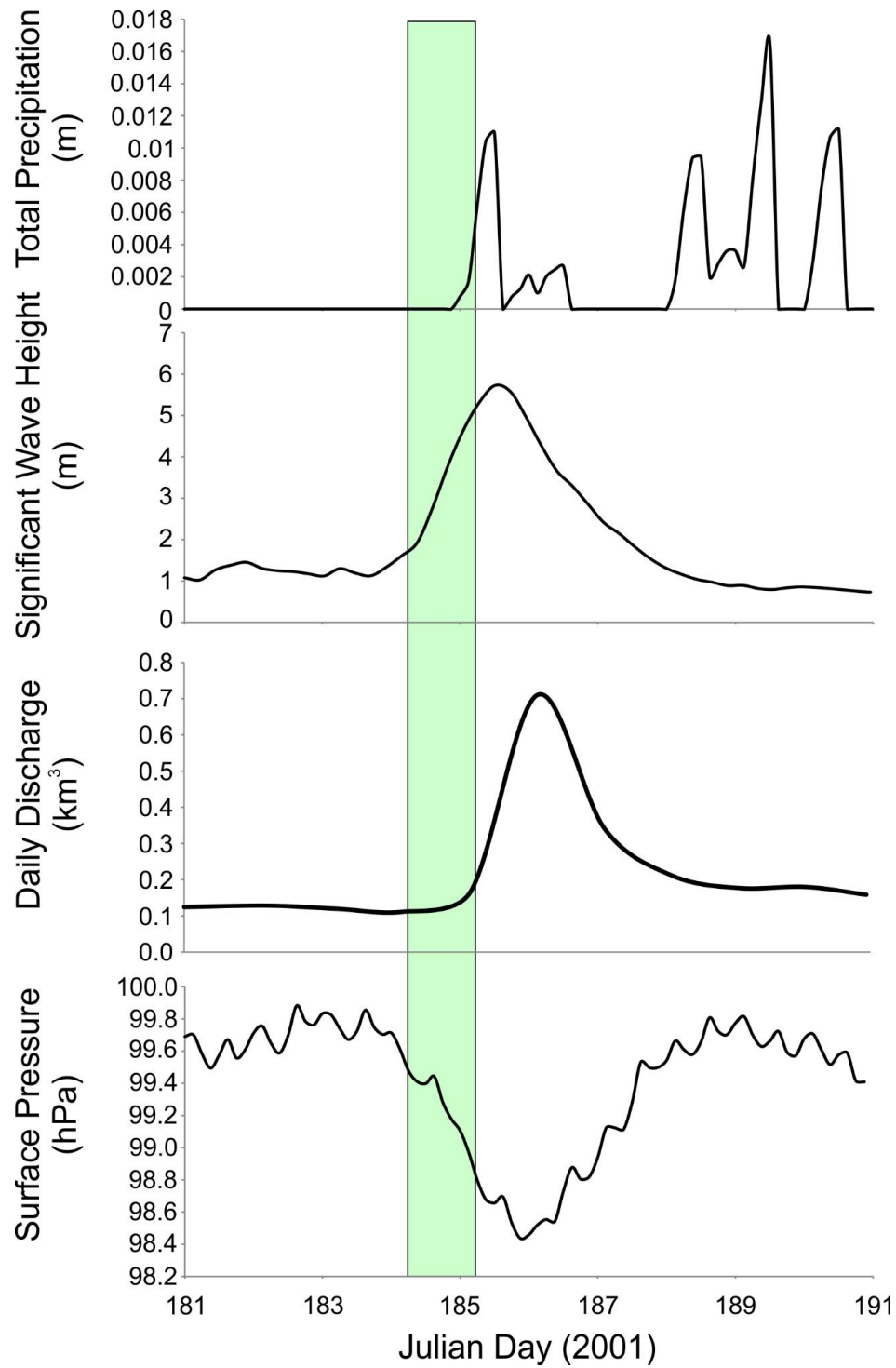


Fig. 4. An example of a Type 1 cable break that is synchronous with typhoon induced wave height increases. Changes in rainfall, wave height and surface air pressure during a tropical cyclone and the relative timing of cable breaks offshore Taiwan in 2001. ERA-Interim data for the cable break occurring offshore Taiwan during the passage of Severe Storm Utor, 2001. Green bar represents the time when the cable broke.

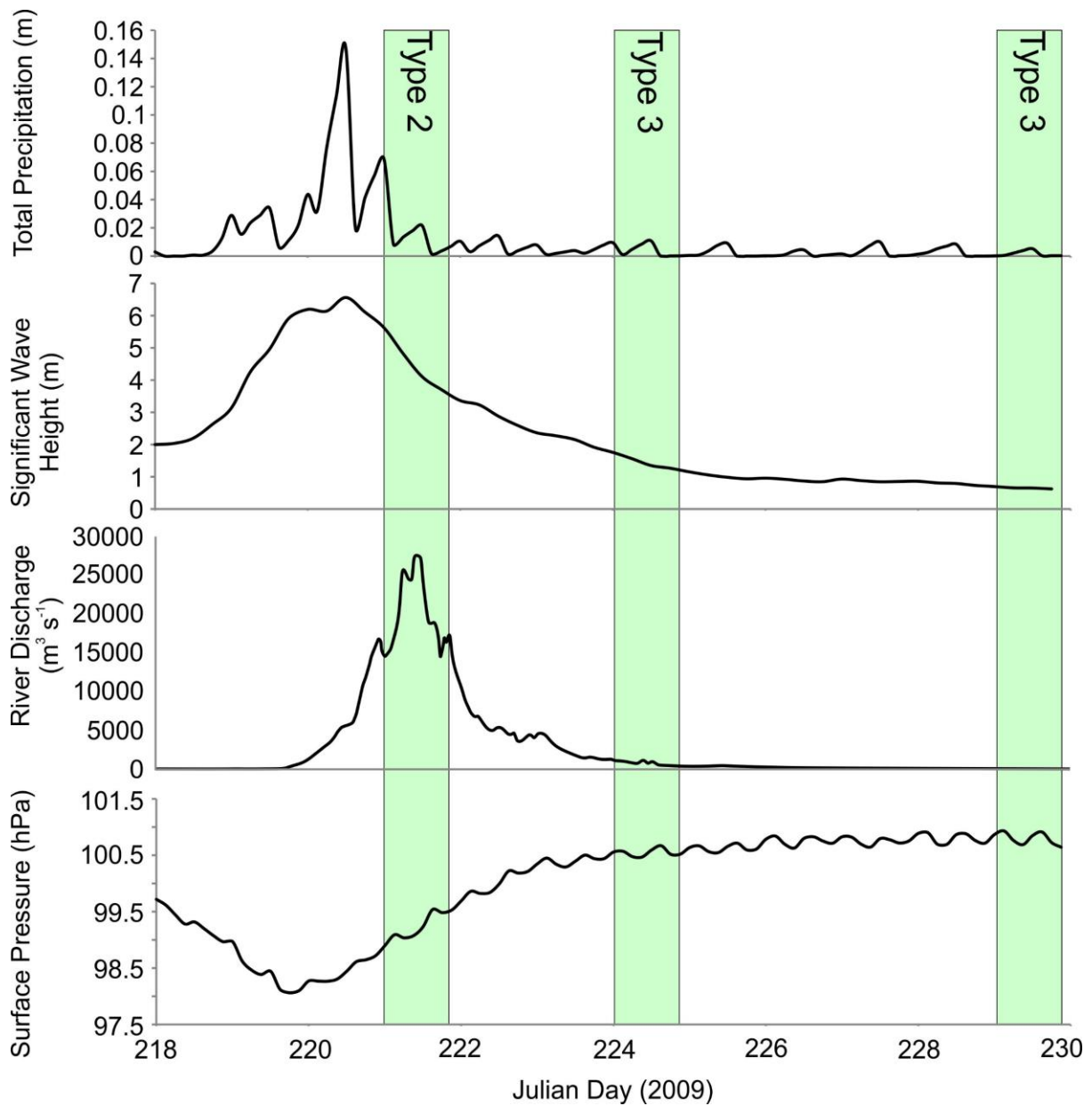


Fig. 5. An example of Type 2 and 3 cable breaks. Environmental conditions for cable breaks occurring at the peak flood discharge resulting from the passing of a tropical cyclone. ERA-Interim data for total precipitation, significant wave height and surface pressure displayed are for offshore Taiwan at the head of the Gaoping Canyon for Typhoon Morakot in 2009. River discharge for the Gaoping River during Typhoon Morakot is also displayed (Carter et al., 2012). Green bars represent the time when cables were broken. The first set of cable breaks represents a Type 2 break. The second and third sets of cable breaks represent Type 3 breaks.

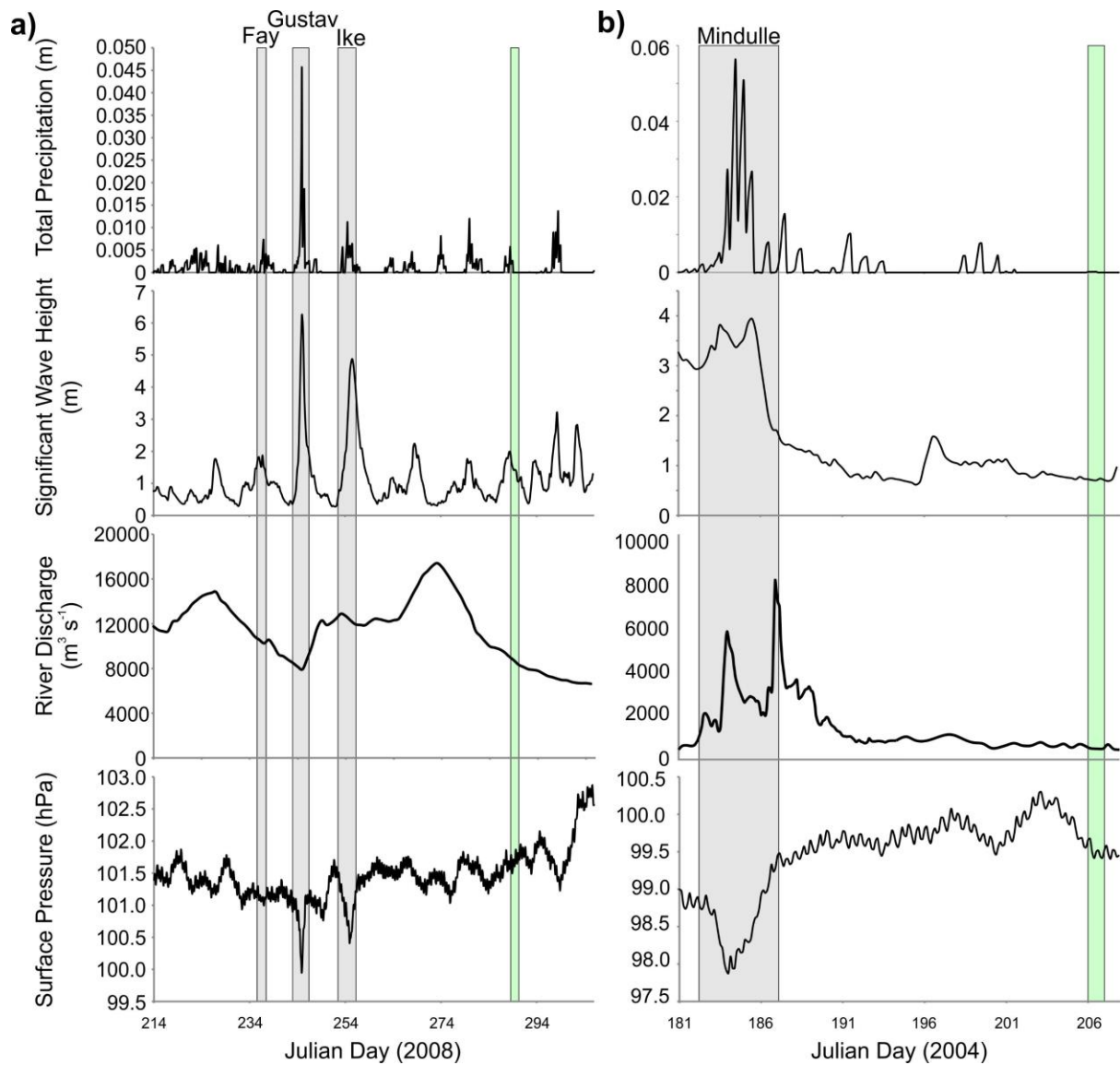
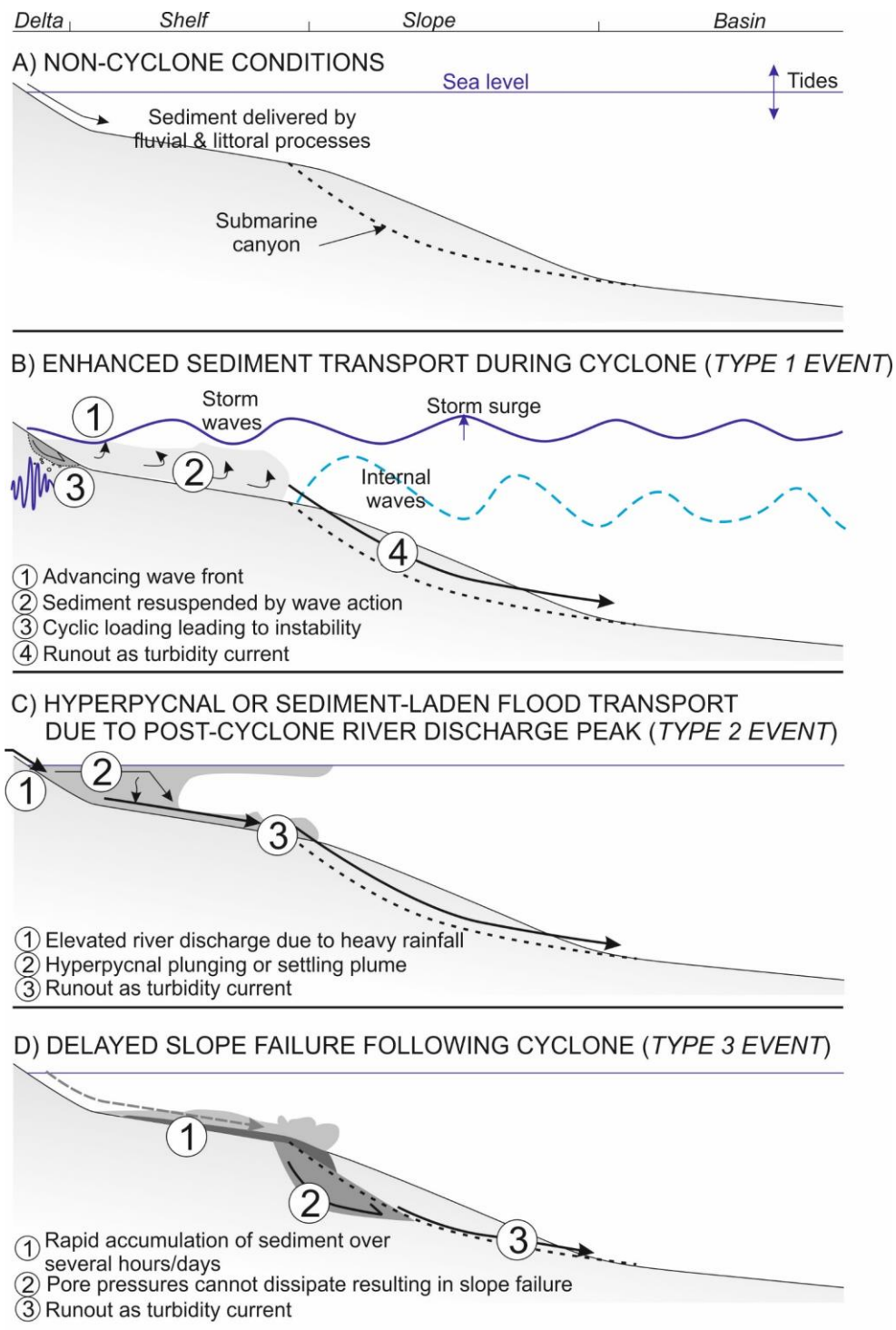


Fig. 6. Examples of Type 3 breaks. Environmental conditions for cable breaks occurring after the reduction in peak flood discharge following the passing of a tropical cyclone. a) ERA-Interim data for total precipitation, significant wave height and surface pressure displayed are for the Mississippi Delta following the passing of Tropical Storm Fay, Hurricane Gustav and Hurricane Ike in 2008. River discharge data is from a river station at Baton Rouge on the Mississippi. b) ERA-interim data for total precipitation, significant wave height and surface pressure displayed are for Taiwan following the passing of Typhoon Mindulle in 2004. River discharge data is from the Choshui River (Lu et al., 2008). Green bar represents the time when the cable break occurred.



509

510 Fig. 7. Illustration of the various hypotheses for the triggering of sediment density flows during and
 511 after cyclones. a) Sediment delivery and transport during non-tropical cyclone conditions. b) Type 1
 512 event triggering mechanisms. c) Type 2 event triggering mechanisms. d) Type 3 event triggering
 513 mechanisms.

Location	Water Depth (m)	Date	Setting	Distance from likely source (km)	Relative Timing	Related Tropical Cyclone	Interpreted Type
Izu-Bonin Ridge	1560	15/06/2005	Continental slope (Possible sediment wave field)	36	Significant wave height peak	Typhoon Nesat	Type 1
La Reunion	1214	19/02/2006	Mafate and Saint-Denis Fans	13	Significant wave height peak Surface pressure trough	Severe Tropical Storm 9	Type 1
Taiwan	1518	03/07/2001	Chilung Canyon	78	Significant wave height rising limb	Severe Tropical Storm Utori	Type 1
Pacific North America	4100	13/09/2000	Deep sea fan	185	Surface Pressure Trough	Hurricane Lane	Type 1
Belize	20	01/11/2011	Open continental shelf	16	Peak runoff	Hurricane Rina	Type 2
Japan	2000	25/09/1996	Boso Canyon	98	Peak discharge	Typhoon Violet	Type 2
La Reunion	903	02/03/2007	Mafate and Saint-Denis Fans	9	Peak discharge	Cyclone Gamede	Type 2
La Reunion		03/03/2007	Mafate and Saint-Denis Fans	10	Peak discharge	Cyclone Gamede	Type 2
La Reunion		04/10/2008	Mafate and Saint-Denis Fans	1	Zone of disturbed weather		Type 2
Philippines	4646	07/10/1993	Cagayan Canyon	210	Peak discharge	Typhoon Kadiang	Type 2
Philippines	1683	07/12/2004	Cagayan Canyon	140	Falling limb of peak discharge	Typhoon Nanmadol	Type 2
Taiwan	5700	12/09/2002	Taitung Canyon	213	Falling limb of peak discharge	Typhoon Sinlaku	Type 2
Taiwan	5500	21/08/2007	Haulien Canyon	126	Rising limb of peak discharge	Typhoon Sepat	Type 2
Taiwan	5200	28/07/2014	Taitung Canyon	187	Peak discharge	Typhoon Matmo	Type 3
Taiwan	2876	09/08/2009	Gaoping Canyon	157	Rising limb of peak discharge	Typhoon Morakot	Type 2
Taiwan	1992	09/08/2009	Gaoping Canyon	117	Falling limb of peak discharge	Typhoon Morakot	Type 2
Taiwan	4440	09/08/2009	Taitung Canyon	145	Falling limb of peak discharge	Typhoon Morakot	Type 2
Jamaica	996	21/09/2004	Yellahs Fan	7	1 after peak discharge	Hurricane Ivan	Type 3
Japan	6120	07/10/2007	Mogi Fan	129	10 days after peak discharge	Typhoon Krosa	Type 3
La Reunion	550	16/02/2009	Mafate and Saint-Denis Fans	9	7 days after peak discharge	Typhoon Gael	Type 3
La Reunion	820	28/10/2006	Mafate and Saint-Denis Fans	4	10 days after peak discharge	Tropical Disturbance 1	Type 3
Madagascar	2897	12/03/2011	Onilahy Canyon	64	14 days after peak discharge	Cyclone Bingiza	Type 3
Mississippi	1541	15/10/2008	Mississippi Fan	104	Hurricanes Fay, Gustav, Ike		Type 3
Philippines	77	30/12/1994	Continental Shelf	40	17 days after peak discharge	Typhoon Axel	Type 3
Taiwan	6024	21/09/2002	Haulien Canyon	135	7 days after peak discharge	Typhoon Sinlaku	Type 3
Taiwan	6000	18/11/2003	Haulien Canyon	170	11 days after peak discharge	Typhoon Melor	Type 3
Taiwan	1516	24/07/2004	Chilung Canyon	73	8 days after peak discharge	Typhoon Mindulle	Type 3
Taiwan	3990	12/08/2009	Gaoping Canyon	384	20 days after peak discharge	Typhoon Morakot	Type 3
Taiwan	4025	12/08/2009	Gaoping Canyon	364	4 days after peak discharge	Typhoon Morakot	Type 3
Taiwan	2646	12/08/2009	Gaoping Canyon	260	4 days after peak discharge	Typhoon Morakot	Type 3
Taiwan	1304	12/08/2009	Gaoping Canyon	110	4 days after peak discharge	Typhoon Morakot	Type 3
Taiwan	3816	13/08/2009	Gaoping Canyon	320	4 days after peak discharge	Typhoon Morakot	Type 3
Taiwan	3800	12/08/2009	Gaoping Canyon	355	4 days after peak discharge	Typhoon Morakot	Type 3
Taiwan	2800	12/08/2009	Gaoping Canyon	218	4 days after peak discharge	Typhoon Morakot	Type 3
Taiwan	5200	17/08/2009	Taitung canyon	170	4 days after peak discharge	Typhoon Morakot	Type 3

515

516 Table 1. Tropical cyclone triggered cable breaks. Depending on setting, the distance from likely
517 source is defined as the approximate distance between the cable break and the canyon head, the
518 river mouth or the shelf edge in the case of those occurring on the continental slope.